THE LID-DRIVEN SQUARE CAVITY FLOW: NUMERICAL SOLUTION WITH A 1024x1024 GRID

Carlos Henrique Marchi
marchi@ufpr.br
Department of Mechanical Engineering
Federal University of Paraná (UFPR)
Curitiba, PR, Brazil

Roberta Suero
robertasuero@demec.ufpr.br
Programa de Pós-Graduação em Métodos Numéricos em Engenharia
Universidade Federal do Paraná (UFPR)
Curitiba, PR, Brasil

Abstract. *The problem of flow inside a square cavity whose lid has a constant velocity is solved. This problem is modeled by Navier-Stokes equations. The numerical model is based on the finite volume method with numerical approximations of second-order accuracy and multiple Richardson extrapolations. The iterative process was repeated until the machine round-off error was reached. This work presents results for 42 variables of interest, and the estimate of their discretization errors, on a grid with 1024x1024 nodes and Reynolds numbers 0.01, 10, 100, 400 and 1000. These results are compares with sixteen sources in the literature. The numerical solutions of this work are the most accurate obtained for this problem to date. The use of multiple Richardson extrapolations reduces the discretization error significantly.*

Keywords: *discretization error, error estimate, CFD, Richardson extrapolation, finite volume.*

1. INTRODUCTION

This work addresses the classical problem (Kawaguti, 1961; Burggraf, 1966; Rubin and Khosla, 1977; Benjamin and Denny, 1979; Ghia, Ghia and Shin, 1982) of laminar flow inside a square cavity whose lid moves at a constant velocity: Fig. 1. This problem is widely employed to evaluate numerical methods and to validate codes for solving Navier-Stokes equations (Botella and Peyret, 1998). Several numerical methods have been used, including finite difference (Kawaguti, 1961; Burggraf, 1966; Rubin and Khosla, 1977; Benjamin and Denny, 1979; Ghia, Ghia and Shin, 1982; Zhang, 2003; Gupta and Kalita, 2005; Bruneau and Saad, 2006); finite volume (Hayase, Humphrey and Greif, 1992); lattice Boltzmann (Hou et al., 1995); and the spectral method (Botella and Peyret, 1998). In addition, a variety of mathematical formulations have been used, including the stream function and vorticity (Kawaguti, 1961; Burggraf, 1966; Rubin and Khosla, 1977; Benjamin and Denny, 1979; Ghia, Ghia and Shin, 1982; Zhang, 2003; Nishida and Satofuka, 1992); the stream function and velocity (Gupta and Kalita, 2005); and Navier-Stokes equations (Hayase, Humphrey and Greif, 1992). The problem considered here is also known as "singular driven cavity" (Botella and Peyret, 1998) because there are two discontinuities in the boundary condition of u, in the corners of the lid: 0 on one side and 1 on the other. In contrast, there is a problem called "regularized driven cavity" (Botella and Peyret, 1998), which does not present discontinuities.

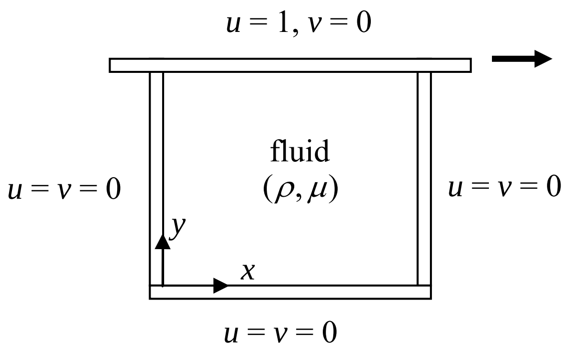

Figure 1. Classical problem of the lid-driven square cavity flow.

The main objective of this work is to present the most accurate numerical solutions found to date for the problem of "singular driven cavity" with Reynolds numbers Re = 0.01, 10, 100, 400 and 1000. To achieve this objective, we use Navier-Stokes equations; the finite volume method; co-located arrangement of variables; segregated solution of the three conservation equations; numerical approximations of second-order accuracy; uniform grid with 1024x1024 control volumes; the iterative process repeated until the machine round-off error is reached; double precision in the calculations; and multiple Richardson extrapolations. Solutions are presented for 42 variables of interest that involve velocity profiles, mass flow rate, minimum value of the stream function, minimum and maximum velocities, and their coordinates, and forces of the walls on the fluid.

Other objectives of this work are: (1) propose an error estimator for use with numerical solutions obtained through multiple Richardson extrapolations; (2) verify (Roache, 1998) if the proposed estimator provides reliable error estimates for a problem whose analytical solution is known (Shih, Tan and Hwang, 1989); (3) apply the proposed estimator to each of the 42 variables of interest and five values of Re, presenting the estimated discretization error of each numerical solution; (4) confirm the order of accuracy of the numerical solutions; and (5) compare the results with sixteen sources in the literature.

Although there is extensive literature on the problem considered here, this work is justified for the following reasons:

- It achieves the main objective proposed.

- It appears that no work has been developed to date to estimate the numerical error involved in the solution of each variable of interest. But this is important in order to know the reliability of numerical solutions, allowing for more careful comparisons to be made.
- Only Bruneau and Saad (2006) and Wright and Gaskell (1995) present solutions on grids as fine as those of the present work, but only for *Re* = 1000, few variables and without using multiple Richardson extrapolations.
- In addition, in the present work, the iterative process is continued until the machine round-off error is reached, which the other authors do not seem to have done.

The next sections discuss the following subjects: the mathematical and numerical models; the theory and equations used to calculate effective and apparent orders of the error, perform multiple Richardson extrapolations, and the discretization error estimator; the results of the problem with known analytical solution; the results of the classical problem; and the conclusion of this work.

2. MATHEMATICAL MODEL

The mathematical model of the problem consists of the Conservation of Mass law and the Conservation of Momentum law (Navier-Stokes equations). The simplifications considered for the problem are: steady state; two-dimensional laminar flow in the x and y directions; incompressible fluid; density (ρ) and viscosity (μ) of the fluid are constant; and without other effects. Thus, the resulting mathematical model is:

$$\frac{\partial u}{\partial x} + \frac{\partial v}{\partial y} = 0 \tag{1}$$

$$\rho\frac{\partial (u^2)}{\partial x} + \rho\frac{\partial (uv)}{\partial y} = \mu\left(\frac{\partial^2 u}{\partial x^2} + \frac{\partial^2 u}{\partial y^2}\right) - \frac{\partial p}{\partial x} \tag{2}$$

$$\rho\frac{\partial (uv)}{\partial x} + \rho\frac{\partial (v^2)}{\partial y} = \mu\left(\frac{\partial^2 v}{\partial x^2} + \frac{\partial^2 v}{\partial y^2}\right) - \frac{\partial p}{\partial y} + S \tag{3}$$

where u and v are the components of the velocity vector in the x and y directions, p is the pressure, and S is a source term. The domain is considered a square of unitary side with the origin of the system of coordinates of Fig. 1.

The variables of interest of the problem involve the primitive variables themselves (u and v), and their averages and integrations. These are:

- Profile of u in $x = ½$ at 15 selected points of y.
- Profile of v in $y = ½$ at 15 selected points of x.
- The minimum value (u_{min}) of the profile of u in $x = ½$ and its respective y coordinate.
- The minimum (v_{min}) and maximum (v_{max}) values of the profile of v in $y = ½$ and their respective x coordinates.
- Minimum value of the stream function (ψ_{min}) and their coordinates x and y.
- The mass flow rate (M) that flows through line $y = ½$ between $x = 0$ and ½ , i.e.,

$$M = \int_0^{1/2} \rho v_{y=1/2}\, z\, dx \tag{4}$$

where z is the depth of the cavity, which is considered unitary.

- The viscous drag force (F) in direction x (Hou et al., 1995) is the force exerted by the surface of the boundary on the fluid, calculated by

$$F = \int_0^1 \mu \left(\frac{\partial u}{\partial y} \right)_y z \, dx \tag{5}$$

where *Fn* is *F* in $y = 1$ (movable lid of the cavity) and *Fs* is *F* in $y = 0$ (lower wall of the cavity).

3. NUMERICAL MODEL

Briefly, the numerical model adopted to solve the mathematical model described by Eqs. (1) to (3) has the following characteristics: (1) finite volume method (Ferziger and Peric, 1999); (2) central difference scheme (CDS) (Ferziger and Peric, 1999) for the diffusive and pressure terms; (3) CDS scheme with deferred correction (Ferziger and Peric, 1999; Khosla and Rubin, 1974) on the upstream difference scheme (UDS) for the advective terms; (4) Eqs. (1) to (3) are solved sequentially using the *MSI* (Modified Strongly Implicit) method (Schneider and Zedan, 1981); (5) SIMPLEC (Semi IMPlicit Linked Equations Consistent) method (Van Doormaal and Raithby, 1984) to treat the pressure-velocity coupling; (6) uniform grids; (7) the boundary conditions for *u* and *v*, Fig. 1, are applied by means of ghost volumes (Ferziger and Peric, 1999); (8) Eqs. (1) to (3) are written for an unsteady state, aiming to use time as a relaxation parameter in the iterative solution process of the discretized mathematical model; and (9) a co-located arrangement of variables is used (Marchi and Maliska, 1994). This numerical model does not require boundary conditions for pressure (Ferziger and Peric, 1999).

The numerical solution of the variables of interest is obtained as follows:

- The numerical solution of the profile of *u* in $x = ½$ is obtained by the arithmetical mean of *u* stored at the east face of the two volumes adjacent to each desired *y* coordinate. This *u* at the east face of each control volume is that of the co-located arrangement of variables of Marchi and Maliska (1994). This is necessary because the number of volumes used in each coordinate direction is even, so that no control volume center coincides with the line $x = ½$.
- The numerical solution of the profile of *v* in $y = ½$ is obtained analogously to the profile of *u*, through the arithmetic mean of *v* stored at the north face of the two volumes adjacent to each desired *x* coordinate.
- u_{min} is the minimum value of the solution of *u* stored at the east face among all the control volumes of the grid with $x = ½$. And its *y* coordinate is that of the center of the east face of the volume corresponding to u_{min}.
- v_{min} and v_{max} are the minimum and maximum values of the solution of *v* stored at the north face among all the control volumes of the grid with $y = ½$. And their *x* coordinates are the ones in the center of the north face of the volume corresponding to v_{min} and v_{max}.
- For each vertical line, the numerical solution of the field of the stream function (ψ) is obtained through the integration of the product of *u*, stored at the east face of each control volume, by the height of each control volume (Δy), starting from the lower wall, in $y = 0$. The vertical lines coincide with the *x* coordinates of the faces of each control volume. The numerical integration used here is of the rectangular rule (Kreyszig, 1999). The minimum value of the stream function (ψ_{min}) is obtained directly from the ψ field.
- The numerical solution of the mass flow rate (*M*) defined by Eq. (4) is obtained by numerical integration by the rectangular rule, through

$$M = z \rho \Delta x \sum_{i=1}^{N_x/2} v_{n,i,y=½} \tag{6}$$

where *i* represents the number of the control volume in the *x* direction; $i = 1$ is the real control volume at the left-hand wall of the cavity; N_x is the total number of real control volumes in the *x* direction; Δx is the width of each control volume; and v_n is v at the north face of each control volume.

- The numerical solution of the force (Fn), which is defined by Eq. (5), is obtained with one upstream point (UDS) (Ferziger and Peric, 1999) and the numerical integration used here is the rectangular rule, which results in

$$Fn = \frac{2z\mu\Delta x}{\Delta y}\sum_{i=1}^{N_X}(u_{T,i} - u_{i,N_Y}) \tag{7}$$

where $u_{T,i}$ is the velocity of the lid of the cavity at the x coordinate of the center of each control volume i; and u_{i,N_Y} is the nodal velocity u at the center of each real control volume i, whose north face of the volume coincides with the lid of the cavity.

- The numerical solution of Fs, defined by Eq. (5), is obtained analogously to Fn but with a point downstream (DDS) (Ferziger and Peric, 1999), resulting in

$$Fs = -\frac{2z\mu\Delta x}{\Delta y}\sum_{i=1}^{N_X} u_{i,1} \tag{8}$$

where $u_{i,1}$ is the nodal velocity u at the center of each real control volume i, whose south face of the volume coincides with the lower wall of the cavity, whose $u = 0$.

The (Stokes 1.5) computational code was implemented in Fortran 95, using Intel Fortran 9.1 software and double precision. The iterative process is repeated until the machine round-off error is reached. This is verified by monitoring the l_1-norm (Kreyszig, 1999), along the iterations, of the sum of the residue of the three systems solved of Eqs. (1) to (3). The value of the sum of the residue of the three systems, in each outer iteration, is nondimensionalized by its value at the end of the first outer iteration.

4. DISCRETIZATION ERROR

The numerical error (E) can be defined as the difference between the exact analytical solution (Φ) of a variable of interest and its numerical solution (ϕ), i.e.,

$$E(\phi) = \Phi - \phi \tag{9}$$

The sources that cause numerical error can be divided into four types (Marchi and Silva, 2002): truncation, iteration, round-off, and programming errors. When other sources of error are inexistent or very minor in relation to truncation errors, the numerical error can also be called as discretization error.

Considering the numerical model described in the previous section, the predicted asymptotic order (p_L) of the discretization error is equal to two (Ferziger and Peric, 1999; Schneider, 2007) for all the variables of interest, except for the x and y coordinates of ψ_{min}, u_{min}, v_{min} and v_{max}, whose p_L are unknown. In the literature (Roache, 1998, 1994), p_L is also called formal order or accuracy order.

In theory (Marchi, 2001), it is expected that p_E (effective order) and p_U (apparent order) $\rightarrow p_L$ for $h \rightarrow 0$. In other words, it is expected that the practical orders (p_E and p_U), which are calculated with the numerical solutions of each variable of interest, tend toward the asymptotic order (p_L), foreseen a priori, when the size of the control volumes (h) tends toward zero.

The effective order (p_E) of the true error is defined by (Marchi, 2001)

$$p_E = \frac{\log\left[\dfrac{E(\phi_2)}{E(\phi_1)}\right]}{\log(r)} \qquad (10)$$

where $E(\phi_1)$ and $E(\phi_2)$ are true discretization errors of the numerical solutions ϕ_1 and ϕ_2 obtained, respectively, with fine (h_1) and coarse (h_2) grids, h = size of the control volumes (in this work, $h = \Delta x = \Delta y$), $r = h_2/h_1$ (grid refinement ratio).

According to Eq. (10), the effective order (p_E) is a function of the true discretization error of the variable of interest. Thus, for problems whose analytical solution is known, it can be used to verify a posteriori if, as $h \to 0$, one obtains p_L. When E is unknown, (p_E) cannot be calculated. In this case, one can use the concept of apparent order (p_U) or observed order defined by (De Vahl Davis, 1983; Marchi and Silva, 2002)

$$p_U = \frac{\log\left(\dfrac{\phi_2 - \phi_3}{\phi_1 - \phi_2}\right)}{\log(r)} \qquad (11)$$

where ϕ_1, ϕ_2 and ϕ_3 = numerical solutions obtained, respectively, with fine (h_1), coarse (h_2) and supercoarse (h_3) grids, and $r = h_3/h_2 = h_2/h_1$.

Some studies (Benjamin and Denny, 1979; Schreiber and Keller, 1983; Erturk, Corke and Gökçöl, 2005) achieved excellent results when employing multiple Richardson extrapolations to reduce the discretization error of ψ_{min}. However, these authors used this process with at most four grids, resulting in up to three extrapolations for the finest grid they used. In the present work, this procedure was utilized with up to ten grids, resulting in up to nine extrapolations for the finest grid used (1024x1024), and applied to almost all the variables of interest. This was done by means of

$$\phi_{1,m\infty} = \phi_{1,(m-1)\infty} + \frac{\phi_{1,(m-1)\infty} - \phi_{2,(m-1)\infty}}{r^{p_V(m)} - 1} \qquad (m = 1, 2, \ldots nm\text{-}1) \qquad (12)$$

where $\phi_{1,m\infty}$ is the numerical solution of the variable of interest (ϕ) with m extrapolations on the fine grid (h_1); $\phi_{1,(m-1)\infty}$ and $\phi_{2,(m-1)\infty}$ are numerical solutions with (m-1) extrapolations on the fine (h_1) and coarse (h_2) grids; $r = h_2/h_1$ (grid refinement ratio); m = number of Richardson extrapolations, with m = 0 being the numerical solution obtained in grid h without any extrapolation; nm = number of different grids with numerical solutions of ϕ without any extrapolation; $p_V(m)$ = true orders (Marchi and Silva, 2002) of the discretization error, with $p_V(1) = p_L$. For the numerical model used in this work, p_V = 2, 4, 6 ... for all the variables of interest, except for the x and y coordinates of ψ_{min}, u_{min}, v_{min} and v_{max}, whose values of p_V are unknown.

In this work, Eq. (12) is applied to all the variables of interest to reduce the discretization error, except to the x and y coordinates of ψ_{min}, u_{min}, v_{min} and v_{max}, whose results are the ones obtained with the finest grid, of 1024x1024 nodes, without any extrapolation. In theory, the accuracy order of the results of u(0.5;05), v(0.5;0.5), M, Fs, Fn, v_{min}, v_{max}, u_{min} and ψ_{min} is 20, since they are obtained with nine extrapolations through Eq. (12). And, in the case of the profiles of u and v, it is 14, because they are obtained with six extrapolations.

In practical situations, a numerical solution is obtained because the analytical solution is unknown. Hence, the true value of the numerical error is also unknown. Therefore, the numerical error must be estimated. The estimated discretization error (U) of $\phi_{1,(nm-1)\infty}$, i.e., of the numerical solution with the highest possible number of extrapolations in the finest grid, will be considered equal to

$$U(\phi_{1,(nm-1)\infty}) \quad = \quad \left|\phi_{1,(nm-2)\infty} - \phi_{2,(nm-2)\infty}\right| \qquad (13)$$

which is the module of the difference with the highest number of extrapolations that can be calculated between the two finest grids. In the case of the x and y coordinates of ψ_{min}, u_{min}, v_{min} and v_{max}, one adopts

$$U(x,y) \quad = \quad \left|\phi_{1024x1024} - \phi_{512x512}\right| \qquad (14)$$

where $\phi_{1024x1024}$ and $\phi_{512x512}$ are the numerical solutions obtained without extrapolation on the grids with 1024x1024 and 512x512 nodes.

The literature (Roache, 1998) offers several discretization error estimators. The use of Eqs. (13) and (14) is justified based on an analysis of the problem presented in the section below. This problem is similar to the classical problem of square cavity with movable lid, but its analytical solution is known. Thus, it was possible to evaluate the performance of Eqs. (13) and (14), which resulted in reliable error estimates, i.e., $U/|E| \geq 1$ for all the variables of interest of the present work.

5. PROBLEM WITH A KNOWN ANALYTICAL SOLUTION

There is a variant of the classical problem whose analytical solution is known and is given by Shih, Tan and Hwang (1989). In this case, the source term (S) of Eq. (3) is different from zero, and is presented in Shih, Tan and Hwang (1989). The analytical solution of u and v is (Shih, Tan and Hwang, 1989)

$$u(x,y) \quad = \quad 8(x^4 - 2x^3 + x^2)(4y^3 - 2y) \qquad (15)$$

$$v(x,y) \quad = \quad -8(4x^3 - 6x^2 + 2x)(y^4 - y^2) \qquad (16)$$

The velocity of the lid varies with x according to Eq. (15) for $y = 1$. The other boundary conditions are shown in Fig. 1. The Reynolds number (Re) is one.

All the numerical solutions in this work were obtained with ten different grids: 2x2, 4x4, 8x8 and so on up to 1024x1024 real control volumes. The microcomputer used in all the simulations of this study is equipped with a Xeon Quad Core X5355 Intel processor, 2.66 GHz and 16 GB of RAM. The results described in this section were obtained with a CPU time of 1 day and 9 hours for the 1024x1024 grid. To obtain the numerical solutions, the initial estimate used for u, v and p was the analytical solution of the problem given, respectively, by Eqs. (15) and (16) and by Shih, Tan and Hwang (1989).

For this problem and the 1024x1024 grid, the l_1-norm of the sum of the residue of the three solved systems, made dimensionless based on the first iteration, reached a value of approximately 2.8×10^{-10}. Ideally, for the model used in this work, the value of the stream function (ψ) in $y = 1$ should be null for each of the 1024 control volumes at the lid of the cavity. Its absolute maximum value, which represents the mass conservation error, resulted in 1.4×10^{-14}.

The velocity profiles in the two directions in the center of the cavity are shown in Fig. 2. The congruence between the analytical solution of Shih, Tan and Hwang (1989) and the numerical solution of the present work, with the 1024x1024 grid, can be considered excellent.

For each variable of interest, Table 1 presents (a) the effective order (p_E), calculated by Eq. (10), based on the true discretization error (E) of the numerical solutions (ϕ) without extrapolation, on the grids with 1024x1024 and 512x512 nodes, i.e., with $r = 2$; (b) the numerical solution (ϕ) on the grid with 1024x1024 nodes, without or with extrapolation calculated by Eq. (12), depending on the variable; (c) the value of E, calculated by Eq. (9); and (d) the ratio of the estimated discretization error (*U*) to the module of *E*. In this table and the following ones, the notation 1.0e-3 and Ind. represent, respectively, $1.0\text{x}10^{-3}$ and indefinite.

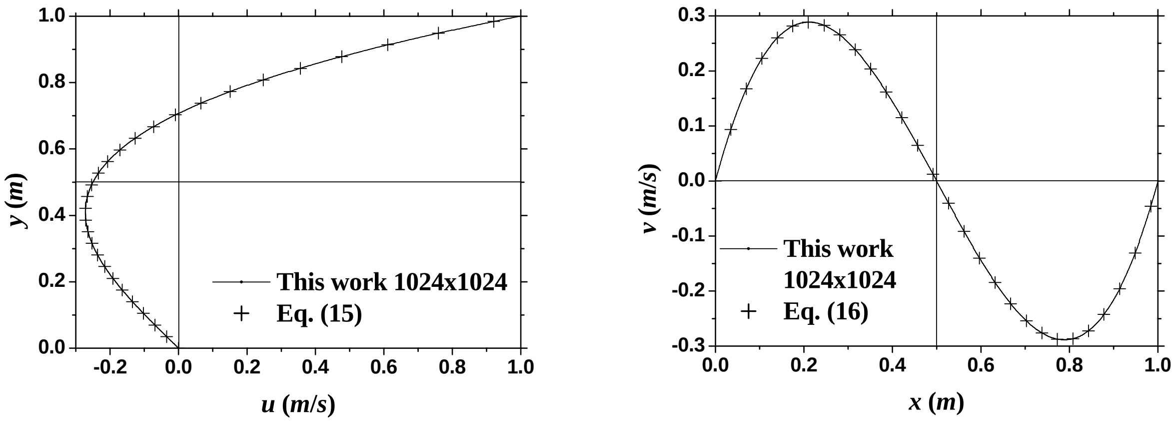

Figure 2. *u* at *x* = ½ and *v* at *y* = ½ for the problem of Shih, Tan and Hwang (1989).

Table 1. Results for the problem of Shih, Tan and Hwang (1989)

Variable	p_E	ϕ	E	$U/\|E\|$
ψmin	1.956996	-1.2500000e-1	2.0e-9	2.4e+2
x(ψmin)	Ind.	5.0e-1	0	Ind.
y(ψmin)	0	7.0703e-1	7.6e-5	6.4
M	2.000252	9.3749999997e-2	2.7e-12	7.4
Fs	1.999764	5.333333334e-1	-8.2e-11	1.8e+1
Fn	1.638635	2.666678e+0	-1.1e-5	3.1
umin	2.082329	-2.721659e-1	3.4e-7	1.1e+1
y(umin)	1.071713	4.0869e-1	-4.4e-4	1.1
vmin	2.583567	-2.886756e-1	4.2e-7	2.6
x(vmin)	2.545598	7.8857e-1	1.0e-4	4.9
vmax	2.566173	2.886756e-1	-4.2e-7	2.6
x(vmax)	2.545598	2.1143e-1	-1.0e-4	4.9
u(0.5;0.0625)	2.000029	-6.2011718741e-2	-8.5e-12	7.3
u(0.5;0.125)	2.000029	-1.21093749988e-1	-1.2e-11	7.3
u(0.5;0.1875)	2.000077	-1.74316406238e-1	-1.2e-11	7.4
u(0.5;0.25)	1.999877	-2.18749999990e-1	-9.8e-12	7.3
u(0.5;0.3125)	1.999951	-2.51464843745e-1	-5.4e-12	7.6
u(0.5;0.375)	1.999963	-2.695312499997e-1	-2.8e-13	1.8e+1
u(0.5;0.4375)	1.999966	-2.70019531254e-1	4.0e-12	6.2
u(0.5;0.5)	1.999965	-2.50000000006e-1	5.9e-12	6.6
u(0.5;0.5625)	1.999963	-2.06542968755e-1	4.6e-12	6.7
u(0.5;0.625)	1.999960	-1.367187500006e-1	6.0e-13	6.7
u(0.5;0.6875)	1.999961	-3.7597656248e-2	-2.0e-12	6.5
u(0.5;0.75)	1.999970	9.3749999998e-2	2.0e-12	9.0
u(0.5;0.8125)	1.999986	2.60253906243e-1	7.2e-12	7.8
u(0.5;0.875)	2.000027	4.64843749987e-1	1.3e-11	7.5
u(0.5;0.9375)	1.995103	7.10449218737e-1	1.3e-11	7.0
v(0.0625;0.5)	1.999920	1.53808593744e-1	6.2e-12	7.1
v(0.125;0.5)	1.999929	2.4609374999e-1	1.4e-11	7.1
v(0.1875;0.5)	1.999935	2.8564453123e-1	1.5e-11	7.3
v(0.25;0.5)	1.999942	2.81249999990e-1	1.0e-11	7.6
v(0.3125;0.5)	1.999952	2.41699218747e-1	3.3e-12	7.6
v(0.375;0.5)	1.999964	1.75781250002e-1	-2.3e-12	6.5
v(0.4375;0.5)	1.999979	9.2285156254e-2	-3.7e-12	6.8
v(0.5;0.5)	1.999762	2.3e-14	-2.3e-14	1.0e+1
v(0.5625;0.5)	1.999963	-9.2285156254e-2	3.6e-12	6.9
v(0.625;0.5)	1.999959	-1.75781250002e-1	2.1e-12	6.2
v(0.6875;0.5)	1.999952	-2.41699218746e-1	-3.5e-12	7.7
v(0.75;0.5)	1.999944	-2.81249999989e-1	-1.1e-11	7.0
v(0.8125;0.5)	1.999938	-2.8564453123e-1	-1.5e-11	7.3
v(0.875;0.5)	1.999934	-2.4609374999e-1	-1.4e-11	7.1
v(0.9375;0.5)	1.999925	-1.53808593744e-1	-5.9e-12	7.1

In Table 1, note that for the velocity profiles of u and v, p_E varies from 1.995 to 2.000, confirming the value of $p_L = 2$, which was predicted a priori. For the coordinate type variables, p_E is indefinite or assumes values of null and close to unity or to two. With the other variables, p_E varies from 1.639 to 2.584, i.e., around p_L.

Table 1 indicates, for all the variables of interest, that $U/|E| \geq 1$ for U calculated by Eqs. (13) or (14), depending on the variable. In other words, the analytical solution is contained within the interval comprised by $\phi \pm U$. For the velocity profiles u and v, the $U/|E|$ ratio varies between 6.2 and 18. For the coordinate type variables, this ratio varies from 1.1 to 6.4. In the case of the other variables, the ratio varies between 2.6 and 240.

For the velocity profiles u and v, M and Fs, the $|Eh/E|$ ratio varies from 1.6×10^3 to 3.8×10^6. This ratio represents the extent to which the discretization error of the solution without extrapolation (Eh), obtained on the 1024x1024 grid, is reduced with the use of multiple extrapolations through Eq. (12). This reduction was not so effective for the variables v_{min}, v_{max}, u_{min}, Fn and ψ_{min}, which reductions were, respectively, of 1.9, 2.0, 2.6, 4.6 and 75.

The magnitude of E and U may vary considerably in the velocity profiles. The ratio between the maximum and minimum values of E is 652, and for U it is 478.

Summarizing, in this section, for a two-dimensional flow problem with a known analytical solution, we showed: (1) the importance of using multiple extrapolations to reduce the true discretization error (E); and (2) the discretization error estimated (U) with Eqs. (13) or (14) is reliable, i.e., $U/|E| \geq 1$. In the next section, the same procedure is applied to the classical cavity flow problem whose analytical solution is unknown.

6. CLASSICAL PROBLEM WITH UNKNOWN ANALYTICAL SOLUTION

In the classical problem (Kawaguti, 1961; Burggraf, 1966; Rubin and Khosla, 1977; Benjamin and Denny, 1979; Ghia, Ghia and Shin, 1982) of laminar flow inside a square cavity, the velocity of the lid (U_T) is constant and has a unitary value. The other boundary conditions are shown in Fig. 1. In the corners of the lid, $u = 0$ on one side and $u = 1$ on the other. The source term (S) of Eq. (3) is null. The Reynolds number (Re) is defined by

$$Re = \rho U_T \frac{L}{\mu} \tag{17}$$

where $L = 1\ m$, dimension of the side of the square cavity; $\rho = 1\ kg/m^3$, density; and μ is the viscosity in $Pa.s$, obtained from Eq. (17) for a given Re.

Numerical solutions were obtained for Re = 0.01, 10, 100, 400 and 1000. The initial estimate used was $u = v = p = 0$. For these five values of Re and the 1024x1024 grid, the CPU time varied from (2 days and 9 hours) to (9 days and 1 hour). The l_1-norm of the sum of the residue of the three solved systems varied from 1.6×10^{-15} to 9.5×10^{-13}. The value of the stream function (ψ) in $y = 1$, which should be null for each of the 1024 control volumes at the lid of the cavity, resulted in the following maximum values: 5.9×10^{-16}, 1.7×10^{-15}, 5.4×10^{-16}, 1.0×10^{-15} and 2.3×10^{-15}, respectively, for Re = 0.01, 10, 100, 400 and 1000.

The velocity profiles in the two directions at the center of the cavity are shown in Fig. 3. The congruence between the numerical solutions of Ghia, Ghia and Shin (1982), Botella and Peyret (1998) and Bruneau and Saad (2006), and the numerical solution of this work, using the 1024x1024 grid, can be considered very good.

Table 2 presents the apparent order (p_U) for Re = 0.01, 10, 100, 400 and 1000. This order was calculated using Eq. (11), based on the numerical solutions (ϕ) of each variable of interest, without extrapolation, on the grids with 1024x1024, 512x512 and 256x256 nodes, i.e., with $r = 2$. For the u and v velocity profiles, p_U varies from 1.760 to 2.345, with most of the results very close to the value of $p_L = 2$, which was predicted a priori. For the coordinate type variables, p_U is indefinite or assumes a unitary value. In the case of the other variables, p_U can differ substantially from p_L, varying from 1.102 to 2.191.

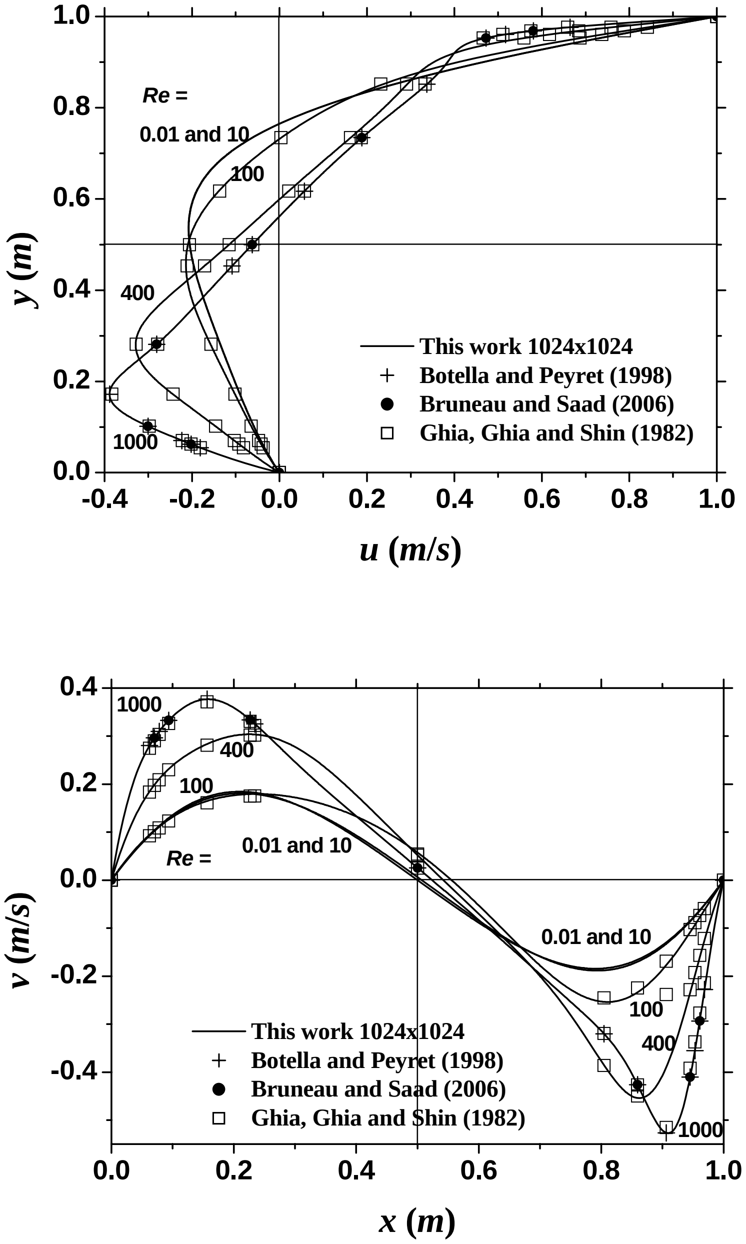

Figure 3. ***u*** **at** ***x*** **= ½ and** ***v*** **at** ***y*** **= ½ for the classical problem.**

An unexpected behavior of p_U, shown in Table 2, occurred for the variable *Fn*. For the five values of *Re*, p_U varies between $-3.50\text{x}10^{-4}$ and $3.06\text{x}10^{-2}$. Based on p_U versus *h* curves, it was found that $p_U \to 0$ for $h \to 0$. This means that the value of *Fn* diverges with the grid refinement. In Nie, Robbins and Chen (2006), for the same problem as that of this work, it was shown that *Fn* cannot be obtained solely through continuum mechanics, i.e., with Navier-Stokes equations. It is necessary to also consider the movement on the microscopic scale. And this problem is due to the discontinuity existing in the boundary condition of *u*, in the corners of the lid: 0 on one side and 1 on the other. In Bruneau and Saad (2006), two other variables were found to diverge when $h \to 0$ due to the discontinuity existing in the boundary condition of *u*. It should be noted that for *Fs*: (a) in the five values of *Re*, its value converges to $h \to 0$; (b) it is calculated with the same types of numerical approximations as *Fn*; (c) its p_U varies from 1.322 to 2.029; and (d) its calculation does not involve discontinuities.

Table 2. Apparent order (p_U) for the classical problem

Variable	Re = 0.01	Re = 10	Re = 100	Re = 400	Re = 1000
ψmin	1.813490	1.329414	1.831320	2.001399	1.995930
x(ψmin)	Ind.	Ind.	Ind.	Ind.	Ind.
y(ψmin)	Ind.	Ind.	Ind.	Ind.	Ind.
M	2.034916	2.028581	1.996948	2.006947	2.002034
Fs	1.992172	1.994006	2.029269	1.332492	1.929611
Fn	-1.59e-6	-9.89e-5	-3.50e-4	5.21e-3	3.06e-2
umin	2.181172	2.066232	2.075970	2.031114	1.997271
y(umin)	1	1	Ind.	Ind.	Ind.
vmin	1.621232	2.190969	1.101600	2.143075	2.125597
x(vmin)	Ind.	1	Ind.	Ind.	1
vmax	1.634400	1.868090	1.997206	2.016770	1.972962
x(vmax)	Ind.	Ind.	Ind.	Ind.	Ind.
u(0.5;0.0625)	1.960768	1.968367	2.147456	1.984548	1.976726
u(0.5;0.125)	1.958143	1.964883	1.868924	1.999443	1.993667
u(0.5;0.1875)	1.923552	1.931919	1.978974	2.004525	2.005013
u(0.5;0.25)	2.178329	2.126091	1.993379	2.007160	2.015676
u(0.5;0.3125)	2.031881	2.026274	1.998071	2.009989	2.014781
u(0.5;0.375)	2.015371	2.013097	2.000054	2.014118	2.017440
u(0.5;0.4375)	2.008997	2.007837	2.000902	2.020004	2.027410
u(0.5;0.5)	2.005441	2.004812	2.000935	2.028634	2.071716
u(0.5;0.5625)	2.002936	2.002602	1.999763	1.988412	1.932956
u(0.5;0.625)	2.000757	2.000613	1.995031	2.003845	1.981615
u(0.5;0.6875)	1.998272	1.998354	2.085979	2.006704	1.991411
u(0.5;0.75)	1.993929	1.994724	2.004496	2.007500	1.996045
u(0.5;0.8125)	1.976978	1.980210	1.996234	2.007477	1.999568
u(0.5;0.875)	2.057222	2.046188	1.986320	2.007307	2.002394
u(0.5;0.9375)	2.019786	2.017118	1.986999	2.009975	2.010322
v(0.0625;0.5)	2.218522	2.029222	1.990425	2.004249	2.005623
v(0.125;0.5)	2.025451	2.012204	1.991731	2.005891	2.004193
v(0.1875;0.5)	2.011352	2.007024	1.993743	2.006560	2.003540
v(0.25;0.5)	2.006277	2.004850	1.996269	2.007214	2.000912
v(0.3125;0.5)	2.003755	2.004056	1.999362	2.007830	1.996139
v(0.375;0.5)	2.002376	2.004485	2.003797	2.007450	1.991814
v(0.4375;0.5)	2.001669	2.008224	2.014244	1.901847	1.978584
v(0.5;0.5)	1.973113	1.972879	1.759938	2.013626	2.345369
v(0.5625;0.5)	2.001658	1.996774	1.981704	2.010731	2.027308
v(0.625;0.5)	2.002371	1.999829	1.992687	2.008691	2.015160
v(0.6875;0.5)	2.003753	2.002233	1.997319	2.007301	2.010284
v(0.75;0.5)	2.006278	2.005644	2.000465	2.005482	2.006818
v(0.8125;0.5)	2.011358	2.012787	2.003962	2.003772	2.009697
v(0.875;0.5)	2.025481	2.043456	2.080131	2.007310	2.004484
v(0.9375;0.5)	2.220438	1.919401	1.988282	2.002781	1.987050

Table 3 presents, for Re = 0.01, 10, 100, 400 and 1000, the numerical solution (ϕ) of each variable of interest. In the case of coordinate type variables, the solution is presented without extrapolations, obtained on the grid with 1024x1024 nodes. For the remaining variables, the solution is the one obtained on the grid with 1024x1024 nodes with extrapolations through Eq. (12). No results are shown for Fn due to its divergence. The number of significant digits presented for each variable is defined by its respective U value from Table 4.

Table 4 presents the discretization error estimated (U) through Eqs. (13) or (14) for the solution of Table 3. As can be seen, for the profiles of u and v, roughly, the magnitude of U grows with Re. In the case of the remaining variables, this influence of Re on U seems to be absent. For the same Re, the magnitude of U differs considerably among the several variables of interest, which can be divided into three distinct sets: (1) U is generally much lower for the profiles of u and v, M and Fs; (2) v_{min}, v_{max}, u_{min} and ψ_{min} have a slightly higher U; and (3) the coordinate type variables have the highest U. The magnitude of U may vary greatly in the velocity profiles: the ratios between the maximum and minimum values of U are 16000, 47, 30, 24 and 97, respectively, for Re = 0.01, 10, 100, 400 and 1000.

Tables 5 to 10 list the results of this work and those of several other authors for the variables of interest, where: [2] = Burggraf (1966); [3] = Rubin and Khosla (1977); [4] = Benjamin and Denny (1979); [5] = Ghia, Ghia and Shin (1982); [6] = Botella and Peyret (1998); [7] = Zhang (2003); [8] = Gupta and Kalita (2005); [9] = Bruneau and Saad (2006); [11] = Hou et al., (1995); [12] = Nishida and Satofuka (1992); [26] = Schreiber and Keller (1983); [27] = Vanka (1986); [28] =

Goyon (1996); [29] = Barragy and Carey (1997); [30] = Wright and Gaskell (1995); and [32] = Erturk, Corke and Gökçöl (2005). Among all the results of the sixteen works reported in the literature and cited here, those of Botella and Peyret (1998) are probably the most accurate. However, considering the estimated error (*U*) reported by Botella and Peyret (1998) and the tolerance they adopted in the iterative process, the results of the present work are probably more accurate than those of Botella and Peyret (1998). Keep in mind that, in the present work, *U* is presented in Table 4 and its value probably overestimates the true error; moreover, the iterative process was repeated until the machine round-off error was reached.

Table 3. Numerical solution (ϕ) for the classical problem

Variable	Re = 0.01	Re = 10	Re = 100	Re = 400	Re = 1000
ψmin	-1.0007622e-1	-1.001132e-1	-1.035212e-1	-1.1398887e-1	-1.18936708e-1
x(ψmin)	5.0000e-1	5.1660e-1	6.1621e-1	5.5371e-1	5.3125e-1
y(ψmin)	7.6465e-1	7.6465e-1	7.3730e-1	6.0547e-1	5.6543e-1
M	5.89511561e-2	5.89995617e-2	6.6547335e-2	1.06628389e-1	1.1651428e-1
Fs	3.20058670e+1	3.19974769e-2	3.2679321e-3	1.1943510e-3	7.980404e-4
umin	-2.077556e-1	-2.075765e-1	-2.140417e-1	-3.287295e-1	-3.885721e-1
y(umin)	5.3564e-1	5.3467e-1	4.5850e-1	2.7979e-1	1.7139e-1
vmin	-1.844491e-1	-1.885062e-1	-2.53804e-1	-4.54058e-1	-5.27056e-1
x(vmin)	7.9053e-1	7.9346e-1	8.1006e-1	8.6182e-1	9.0967e-1
vmax	1.844415e-1	1.809117e-1	1.79572814e-1	3.0383231e-1	3.769471e-1
x(vmax)	2.0947e-1	2.1240e-1	2.3682e-1	2.2510e-1	1.5771e-1
u(0.5;0.0625)	-3.85275436e-2	-3.85425800e-2	-4.1974991e-2	-9.259926e-2	-2.02330048e-1
u(0.5;0.125)	-6.9584425e-2	-6.96238561e-2	-7.7125399e-2	-1.78748051e-1	-3.478451e-1
u(0.5;0.1875)	-9.6906717e-2	-9.6983962e-2	-1.09816214e-1	-2.6391720e-1	-3.844094e-1
u(0.5;0.25)	-1.22595555e-1	-1.22721979e-1	-1.41930064e-1	-3.2122908e-1	-3.189461e-1
u(0.5;0.3125)	-1.47461728e-1	-1.47636199e-1	-1.72712391e-1	-3.2025109e-1	-2.456937e-1
u(0.5;0.375)	-1.71067124e-1	-1.71260757e-1	-1.98470859e-1	-2.6630635e-1	-1.837321e-1
u(0.5;0.4375)	-1.91535923e-1	-1.91677043e-1	-2.12962392e-1	-1.9073056e-1	-1.2341046e-1
u(0.5;0.5)	-2.05191715e-1	-2.05164738e-1	-2.091491418e-1	-1.15053628e-1	-6.205613e-2
u(0.5;0.5625)	-2.06089397e-1	-2.05770198e-1	-1.82080595e-1	-4.2568947e-2	5.6180e-4
u(0.5;0.625)	-1.85581148e-1	-1.84928116e-1	-1.31256301e-1	3.024302e-2	6.5248742e-2
u(0.5;0.6875)	-1.322092275e-1	-1.313892353e-1	-6.0245594e-2	1.0545601e-1	1.3357257e-1
u(0.5;0.75)	-3.2443684e-2	-3.1879308e-2	2.7874448e-2	1.8130685e-1	2.0791461e-1
u(0.5;0.8125)	1.27054983e-1	1.26912095e-1	1.40425325e-1	2.5220384e-1	2.884424e-1
u(0.5;0.875)	3.55228331e-1	3.54430364e-1	3.1055709e-1	3.1682969e-1	3.625454e-1
u(0.5;0.9375)	6.51176326e-1	6.50529292e-1	5.97466694e-1	4.69580199e-1	4.229321e-1
v(0.0625;0.5)	9.4572847e-2	9.2970121e-2	9.4807616e-2	1.85132290e-1	2.807057e-1
v(0.125;0.5)	1.55984965e-1	1.52547843e-1	1.4924300e-1	2.6225126e-1	3.650418e-1
v(0.1875;0.5)	1.82641889e-1	1.78781456e-1	1.74342933e-1	2.9747923e-1	3.678527e-1
v(0.25;0.5)	1.78849493e-1	1.76415100e-1	1.79243328e-1	3.0096003e-1	3.0710428e-1
v(0.3125;0.5)	1.51784706e-1	1.52055820e-1	1.69132064e-1	2.6831096e-1	2.3126839e-1
v(0.375;0.5)	1.089092434e-1	1.121477612e-1	1.45730201e-1	2.0657139e-1	1.6056422e-1
v(0.4375;0.5)	5.66144697e-2	6.21048147e-2	1.087758646e-1	1.30571694e-1	9.296931e-2
v(0.5;0.5)	6.3677058e-6	6.3603620e-3	5.7536559e-2	5.2058082e-2	2.579946e-2
v(0.5625;0.5)	-5.66033951e-2	-5.10417285e-2	-7.748504e-3	-2.4714514e-2	-4.184068e-2
v(0.625;0.5)	-1.089027070e-1	-1.056157259e-1	-8.4066715e-2	-1.00884164e-1	-1.107983e-1
v(0.6875;0.5)	-1.51784274e-1	-1.51622101e-1	-1.63010143e-1	-1.82109238e-1	-1.816797e-1
v(0.75;0.5)	-1.78854716e-1	-1.81633561e-1	-2.27827313e-1	-2.80990219e-1	-2.533815e-1
v(0.8125;0.5)	-1.82650133e-1	-1.87021651e-1	-2.53768577e-1	-4.0004235e-1	-3.315667e-1
v(0.875;0.5)	-1.55992321e-1	-1.59898186e-1	-2.18690812e-1	-4.4901185e-1	-4.677756e-1
v(0.9375;0.5)	-9.4576294e-2	-9.6409942e-2	-1.23318170e-1	-2.70354943e-1	-4.5615254e-1

Among all the variables of interest compared in Tables 5 to 10, the results of Botella and Peyret (1998) are probably more accurate than those of the present work only in the following variables: v_{min} in *Re* = 100 and 1000; and v_{max} in *Re* = 1000. It is worth noting the congruence among all the results of the present work, which are compared to those of Botella and Peyret (1998). The results of Botella and Peyret (1998) lie within the interval comprised between $\phi \pm U$ of the results of this work. For example, the result of Botella and Peyret (1998) for v_{max} in *Re* = 1000 is 0.3769447, which is between 0.3769398 and 0.3769544 of the present work. An exception is ψ_{min}, for which Botella and Peyret (1998) reports a result of −0.1189366, which is not comprised within the interval of −0.118936739 to −0.118936677 of the present work, presenting a very slight difference of $7.7 \text{x} 10^{-8}$.

Table 4. Estimated discretization error (*U*) of the numerical solution (ϕ) for the classical problem.

Variable	Re = 0.01	Re = 10	Re = 100	Re = 400	Re = 1000
ψmin	3.5e-7	1.5e-6	1.1e-6	3.1e-7	3.1e-8
x(ψmin)	4.9e-4	9.8e-4	9.8e-4	9.8e-4	4.9e-4
y(ψmin)	9.8e-4	9.8e-4	9.8e-4	4.9e-4	9.8e-4
M	9.3e-9	8.3e-9	2.7e-8	8.6e-8	5.8e-7
Fs	7.0e-6	7.8e-9	5.8e-9	8.0e-9	8.8e-9
umin	1.7e-6	1.3e-6	1.6e-6	1.1e-6	3.8e-6
y(umin)	4.9e-4	4.9e-4	4.9e-4	4.9e-4	4.9e-4
vmin	1.9e-6	2.2e-6	1.1e-5	2.1e-5	6.2e-5
x(vmin)	4.9e-4	4.9e-4	4.9e-4	4.9e-4	4.9e-4
vmax	1.8e-6	1.1e-6	2.7e-8	2.5e-7	7.3e-6
x(vmax)	4.9e-4	4.9e-4	4.9e-4	4.9e-4	4.9e-4
u(0.5;0.0625)	5.8e-9	4.8e-9	4.5e-8	1.9e-7	5.4e-8
u(0.5;0.125)	1.1e-8	9.0e-9	7.2e-8	5.6e-8	1.7e-6
u(0.5;0.1875)	1.5e-8	1.3e-8	8.6e-8	2.6e-7	2.1e-6
u(0.5;0.25)	2.0e-8	1.7e-8	8.6e-8	5.0e-7	1.6e-6
u(0.5;0.3125)	2.4e-8	2.1e-8	7.3e-8	4.7e-7	1.4e-6
u(0.5;0.375)	2.8e-8	2.5e-8	5.0e-8	2.8e-7	1.2e-6
u(0.5;0.4375)	3.0e-8	2.8e-8	2.0e-8	1.2e-7	9.4e-7
u(0.5;0.5)	3.0e-8	2.8e-8	8.6e-9	2.7e-8	6.4e-7
u(0.5;0.5625)	2.4e-8	2.3e-8	2.8e-8	5.0e-8	3.6e-7
u(0.5;0.625)	1.2e-8	1.2e-8	3.5e-8	1.2e-7	3.7e-8
u(0.5;0.6875)	7.4e-9	6.4e-9	3.7e-8	2.2e-7	3.4e-7
u(0.5;0.75)	3.2e-8	2.9e-8	4.6e-8	3.2e-7	7.8e-7
u(0.5;0.8125)	5.4e-8	4.9e-8	7.1e-8	3.8e-7	1.4e-6
u(0.5;0.875)	6.1e-8	5.6e-8	1.1e-7	3.3e-7	2.3e-6
u(0.5;0.9375)	4.1e-8	3.9e-8	9.5e-8	2.3e-8	3.6e-6
v(0.0625;0.5)	2.4e-8	2.0e-8	7.2e-8	6.5e-8	2.9e-6
v(0.125;0.5)	3.6e-8	2.9e-8	1.0e-7	1.9e-7	3.0e-6
v(0.1875;0.5)	3.5e-8	2.8e-8	9.7e-8	3.1e-7	1.9e-6
v(0.25;0.5)	2.6e-8	2.2e-8	7.9e-8	3.5e-7	8.6e-7
v(0.3125;0.5)	1.6e-8	1.5e-8	5.5e-8	2.8e-7	4.0e-7
v(0.375;0.5)	7.6e-9	9.2e-9	2.9e-8	1.5e-7	1.1e-7
v(0.4375;0.5)	2.8e-9	5.9e-9	3.7e-9	4.5e-8	2.2e-7
v(0.5;0.5)	3.7e-12	3.8e-9	2.0e-8	2.7e-8	5.2e-7
v(0.5625;0.5)	2.8e-9	1.2e-9	4.8e-8	7.3e-8	7.8e-7
v(0.625;0.5)	7.6e-9	3.9e-9	5.3e-8	9.4e-8	1.0e-6
v(0.6875;0.5)	1.6e-8	1.3e-8	5.0e-8	8.0e-8	1.2e-6
v(0.75;0.5)	2.6e-8	2.4e-8	5.2e-8	7.7e-8	1.5e-6
v(0.8125;0.5)	3.5e-8	3.4e-8	7.3e-8	3.7e-7	1.7e-6
v(0.875;0.5)	3.6e-8	3.6e-8	8.7e-8	5.5e-7	1.9e-6
v(0.9375;0.5)	2.4e-8	2.4e-8	5.8e-8	7.3e-8	5.9e-7

7. CONCLUSION

In this work, a numerical solution was obtained for the laminar flow inside a square cavity whose lid moves at a variable velocity and whose analytical solution is known (Shih, Tan and Hwang, 1989). Results were presented for 42 variables of interest (ϕ) and a grid with 1024x1024 nodes. It was found that:

1) For all the variables of interest, the discretization error estimated (*U*) with Eqs. (13) and (14), proposed here, is reliable, in other words, $U/|E| \geq 1$, where *E* is the true discretization error.
2) The use of multiple Richardson extrapolations with Eq. (12) reduced *E* between $1.6 \text{x} 10^3$ and $3.8 \text{x} 10^6$ times for the velocity profiles *u* and *v*, *M* and *Fs*. This reduction was not so effective for the variables v_{min}, v_{max}, u_{min}, *Fn* and ψ_{min}, which reductions were of 1.9, 2.0, 2.6, 4.6 and 75 times, respectively. For coordinate type variables, this procedure does not apply.
3) For 34 variables, the effective order (p_E) is very close (1.96 to 2.08) to the theoretical value of the asymptotic order (p_L) = 2 predicted a priori. For the coordinate type variables, p_E seems to tend towards unity. In the case of the other variables, p_E varies from 1.64 to 2.58, i.e., around p_L.

The main focus of this work was to solve the problem of laminar flow inside a square cavity whose lid moves at a constant velocity and whose analytical solution is unknown (Kawaguti, 1961; Burggraf, 1966; Rubin and Khosla, 1977; Benjamin and Denny, 1979; Ghia, Ghia and Shin, 1982). Results were presented for 42 variables of interest (ϕ), and their estimated discretization errors (*U*) on a grid of 1024x1024 nodes and Reynolds numbers (Re) = 0.01, 10, 100, 400 and 1000. It was found that:

Table 5. Comparisons of ψ_{min} with other authors for the classical problem

Work	Re = 100			Re = 400			Re = 1000		
	$-\psi_{min}$	x	y	$-\psi_{min}$	x	y	$-\psi_{min}$	x	y
[2]	0.1022			0.1017					
[3]	0.1034						0.114		
[4]							0.1193		
[5]	0.103423	0.6172	0.7344	0.113909	0.5547	0.6055	0.117929	0.5313	0.5625
[26]	0.10330	0.61667	0.74167	0.11399	0.55714	0.60714	0.11894	0.52857	0.56429
[27]	0.1034	0.6188	0.7375	0.1136	0.5563	0.6000	0.1173	0.5438	0.5625
[12]	0.103506	0.6094	0.7344				0.119004	0.5313	0.5625
[11]	0.1030	0.6196	0.7373	0.1121	0.5608	0.6078	0.1178	0.5333	0.5647
[30]	0.103519	0.6157	0.7378				0.118821	0.5308	0.5659
[28]							0.1157		
[29]	0.10330			0.11389			0.118930		
[6]							0.1189366	0.5308	0.5652
[7]	0.103511	0.617187	0.734375				0.118806	0.531250	0.562500
[8]	0.103	0.6125	0.7375	0.113	0.5500	0.6125	0.117	0.5250	0.5625
[32]							0.118942	0.5300	0.5650
[9]							0.11892	0.53125	0.56543
Present	0.1035212	0.61621	0.73730	0.11398887	0.55371	0.60547	0.118936708	0.53125	0.56543

Re = 10: [2] $-\psi_{min}$ = 0.0999; Present: $-\psi_{min}$ = 0.1001132

Table 6. Comparisons of u(0.5;0.5) and v(0.5;0.5) with other authors for the classical problem

Work	u(0.5;0.5)			v(0.5;0.5)		
	Re = 100	Re = 400	Re = 1000	Re = 100	Re = 400	Re = 1000
[5]	-0.20581	-0.11477	-0.06080	0.05454	0.05186	0.02526
[6]			-0.0620561			0.0257995
[32]			-0.0620			0.0258
[9]			-0.06205			0.02580
Present	-0.2091491418	-0.115053628	-0.06205613	0.057536559	0.052058082	0.02579946

Table 7. Comparisons of u(0.5;0.0625) and v(0.0625;0.5) with other authors for the classical problem

Work	u(0.5;0.0625)			v(0.0625;0.5)		
	Re = 100	Re = 400	Re = 1000	Re = 100	Re = 400	Re = 1000
[5]	-0.04192	-0.09266	-0.20196	0.09233	0.18360	0.27485
[6]			-0.2023300			0.2807056
[9]			-0.20227			
Present	-0.041974991	-0.09259926	-0.202330048	0.094807616	0.185132290	0.2807057

Table 8. Comparisons of u_{min} with other authors for the classical problem

Work	Re = 100		Re = 400		Re = 1000	
	u_{min}	y	u_{min}	y	u_{min}	y
[5]	-0.21090	0.4531	-0.32726	0.2813	-0.38289	0.1719
[27]	-0.213	0.4578	-0.327	0.2797	-0.387	0.1734
[6]	-0.2140424	0.4581			-0.3885698	0.1717
Present	-0.2140417	0.45850	-0.3287295	0.27979	-0.3885721	0.17139

Table 9. Comparisons of v_{min} with other authors for the classical problem

Work	Re = 100		Re = 400		Re = 1000	
	v_{min}	x	v_{min}	x	v_{min}	x
[5]	-0.24533	0.8047	-0.44993	0.8594	-0.51550	0.9063
[6]	-0.2538030	0.8104			-0.5270771	0.9092
Present	-0.253804	0.81006	-0.454058	0.86182	-0.527056	0.90967

Table 10. Comparisons of v_{max} with other authors for the classical problem

Work	Re = 100		Re = 400		Re = 1000	
	v_{max}	x	v_{max}	x	v_{max}	x
[5]	0.17527	0.2344	0.30203	0.2266	0.37095	0.1563
[6]	0.1795728	0.2370			0.3769447	0.1578
Present	0.179572814	0.23682	0.30383231	0.22510	0.3769471	0.15771

4) Among all the results of the sixteen works reported in the literature and cited here, those of Botella and Peyret (1998) are probably the most accurate. However, considering the estimated error (U) reported by Botella and Peyret (1998) and the tolerance they adopted in the iterative process, the results of the present work are probably more accurate than those of Botella and Peyret (1998). Among all the variables of interest compared in Tables 5 to 10, the results of Botella and Peyret (1998) are probably more accurate than those of the present work only for the following variables: v_{min} in Re = 100 and 1000; and v_{max} in Re = 1000. There is a notable consistency among all the results of the present work that are compared with those of Botella and Peyret (1998): the results of Botella and Peyret (1998) fall inside the interval comprised between $\phi \pm U$ of the results of the present work.
5) For the velocity profiles u and v, the apparent order (p_U) varies from 1.76 to 2.34, with most of the results very close to the theoretical value of $p_L = 2$ which was predicted a priori. For the coordinate type variables, p_U seems to tend towards unity. In only five cases out of more than 200, the value of p_U varied from 1.10 to 1.63, remaining distant from p_L. An exception is the variable Fn: its value does not converge with the grid refinement, causing p_U to tend towards zero. This is apparently due to the discontinuity in the boundary condition (B.C.) of u in the corners of the lid. In the case of Fs, which does not present discontinuities in the B.C., the solution converges with the grid refinement, with p_U varying from 1.33 to 2.03 for the five values of Re.

Acknowledgments

The second author gratefully acknowledges the support provided by the Laboratory of Numerical Experimentation (LENA), Federal University of Paraná (UFPR), and the guidance of Professors Carlos Henrique Marchi and Fábio Alencar Schneider, as well as CAPES (Coordenação de Aperfeiçoamento de Pessoal de Nível Superior) – Brazil for granting a scholarship. The first author is scholarship of CNPq (Conselho Nacional de Desenvolvimento Científico e Tecnológico) – Brazil. The authors acknowledge The "UNIESPAÇO Program" of The Brazilian Space Agency (AEB).

REFERENCES

Barragy, E. and Carey, G.F., 1997, "Stream Function-Vorticity Driven Cavity Solution Using p Finite Elements", Computers & Fluids, Vol.26, pp. 453-468.

Benjamin, A.S. and Denny, V.E., 1979, “On the Convergence of Numerical Solutions for 2-D Flows in a Cavity at Large Re”, Journal of Computational Physics, Vol.33, pp. 340-358.

Botella, O. and Peyret, R., 1998, “Benchmark Spectral Results on the Lid-Driven Cavity Flow”, Computers & Fluids, Vol.27, pp. 421-433.

Bruneau, C.H. and Saad, M., 2006, “The 2D Lid-Driven Cavity Problem Revisited”, Computers & Fluids, Vol.35, pp. 326-348.

Burggraf, O.R., 1966, “Analytical and Numerical Studies of the Structure of Steady Separated Flows”, J. Fluid Mech., Vol.24, pp. 113-151.

De Vahl Davis, G., 1983, “Natural Convection of Air in a Square Cavity: a Bench Mark Numerical Solution”, International Journal for Numerical Methods in Fluids, Vol.3, pp. 249-264.

Erturk, E., Corke, T.C. and Gökçöl, C, 2005, “Numerical Solutions of 2-D Steady Incompressible Driven Cavity Flow at High Reynolds Numbers”, Int. J. Numer. Meth. Fluids, Vol.48, pp. 747-774.

Ferziger, J.H. and Peric, M., 1999, “Computational Methods for Fluid Dynamics”, Springer-Verlag, Berlin, Germany, 2 ed., 389 p.

Ghia, U., Ghia, K.N. and Shin, C.T., 1982, “High-Re Solutions for Incompressible Flow Using the Navier-Stokes Equations and a Multigrid Method”, Journal of Computational Physics, Vol.48, pp. 387-411.

Goyon, O., 1996, “High-Reynolds Number Solutions of Navier-Stokes Equations Using Incremental Unknowns”, Computer Methods in Applied Mechanics and Engineering, Vol.130, pp. 319-335.

Gupta, M.M. and Kalita, J.C., 2005, “A New Paradigm for Solving Navier-Stokes Equations: Streamfunction-Velocity Formulation”, Journal of Computational Physics, Vol.207, pp. 52-68.

Hayase, T., Humphrey, J.A. and Greif, R., 1992, “A Consistently Formulated QUICK Scheme for Fast and Stable Convergence Using Finite-Volume Iterative Calculation Procedures”, Journal of Computational Physics, Vol.98, pp. 108-118.

Hou, S., Zou, Q., Chen, S., Doolen, G. and Cogley, A.C., 1995, “Simulation of Cavity Flow by Lattice Boltzmann Method”, Journal of Computational Physics, Vol.118, pp. 329-347.

Kawaguti, M., 1961, “Numerical Solution of the Navier-Stokes Equations for the Flow in a Two-Dimensional Cavity”, Journal of The Physical Society of Japan, Vol.16, pp. 2307-2315.

Khosla, P.K. and Rubin, S.G., 1974, “A Diagonally Dominant Second-Order Accurate Implicit Scheme”, Computers & Fluids, Vol.2, pp. 207-209.

Kreyszig, E., 1999, “Advanced Engineering Mathematics”, Wiley, New York, United States of America, 8 ed., 1156 p.

Marchi, C.H., 2001, “Verification of Unidimensional Numerical Solutions in Fluid Dynamics” (in Portuguese), Ph.D. thesis, The Federal University of Santa Catarina, Florianópolis, Brazil, 289 p.

Marchi, C.H. and Maliska, C.R., 1994, “A Nonorthogonal Finite-Volume Method for the Solution of All Speed Flows Using Co-Located Variables”, Numerical Heat transfer, Part B, Vol.26, pp. 293-311.

Marchi, C. H. and Silva, A.F.C., 2002, “Unidimensional Numerical Solution Error Estimation for Convergent Apparent Order”, Numerical Heat Transfer, Part B, Vol.42, pp. 167-188.

Nie, X., Robbins, M.O. and Chen, S., 2006, “Resolving Singular Forces in Cavity Flow: Multiscale Modeling from Atomic to Millimeter Scales”, Physical Review Letters, Vol.96(134501), pp. 1-4.

Nishida, H. and Satofuka, N., 1992, “Higher-Order Solutions of Square Driven Cavity Flow Using a Variable-Order Multi-Grid Method”, International Journal for Numerical Methods in Engineering, Vol.34, pp. 637-653.

Roache, P.J., 1994, “Perspective: a Method for Uniform Reporting of Grid Refinement Studies”, ASME Journal of Fluids Engineering, Vol.116, pp. 405-413.

Roache, P.J., 1998, “Verification and Validation in Computational Science and Engineering”, Hermosa, Albuquerque, United States of America, 446 p.

Rubin, S.G. and Khosla, P.K., 1977, “Polynomial Interpolation Methods for Viscous Flow Calculations”, Journal of Computational Physics, Vol.24, pp. 217-244.

Schneider, F.A., 2007, “Verification of Numerical Solutions in Diffusive and Advective Problems with Nonuniform Grids” (in Portuguese), Ph.D. thesis, The Federal University of Paraná, Curitiba, Brazil, 223 p.

Schneider, G.E. and Zedan, M., 1981, “A Modified Strongly Implicit Procedure for the Numerical Solution of Field Problems”, Numerical Heat transfer, Vol.4, pp. 1-19.

Schreiber, R. and Keller, H.B., 1983, “Driven Cavity Flows by Efficient Numerical Techniques”, Journal of Computational Physics, Vol.49, pp. 310-333.

Shih, T.M., Tan, C.H. and Hwang, B.C., 1989, “Effects of Grid Staggering on Numerical Schemes”, International Journal for Numerical Methods in Fluids, Vol.9, pp. 193-212.

Van Doormaal, J.P. and Raithby, G.D., 1984, “Enhancements of the SIMPLE Method for Predicting Incompressible Fluid Flow”, Numerical Heat transfer, Vol.7, pp. 147-163.

Vanka, S.P., 1986, “Block-Implicit Multigrid Solution of Navier-Stokes Equations in Primitive Variables”, Journal of Computational Physics, Vol.65, pp. 138-158.

Wright, N.G. and Gaskell, P.H., 1995, “An Efficient Multigrid Approach to Solving Highly Recirculating Flows”, Computers & Fluids, Vol.24, pp. 63-79.

Zhang, J., 2003, “Numerical Simulation of 2D Square Driven Cavity Using Fourth-Order Compact Finite Difference Schemes”, Computers and Mathematics with Applications, Vol.45, pp. 43-52.